possibility that selection bias might have led to an apparent differential elimination of regulatory mechanisms. Such an artefact could have occurred if mutant CaMs variably inhibited facilitation, inactivation, or both—depending on the particular cell under observation. Appropriate changes (or lack thereof) in *f* and *g* values, as determined from the same cells, excluded such a scenario (Fig. 4; see Supplementary Information).

Received 14 December 2000; accepted 30 March 2001.

1. Borst, J. G. & Sakmann, B. Facilitation of presynaptic calcium currents in the rat brainstem. *J. Physiol. (Lond.)* **513,** 149–155 (1998).
2. Cuttle, M. F., Tsujimoto, T., Forsythe, I. D. & Takahashi, T. Facilitation of the presynaptic calcium current at an auditory synapse in rat brainstem. *J. Physiol. (Lond.)* **512,** 723–729 (1998).
3. Forsythe, I. D., Tsujimoto, T., Barnes-Davies, M., Cuttle, M. & Takahashi, T. Inactivation of presynaptic calcium current contributes to synaptic depression at a fast central synapse. *Neuron* **20,** 797–807 (1998).
4. Abbott, L. F., Varela, J. A., Sen, K. & Nelson, S. B. Synaptic depression and cortical gain control. *Science* **175,** 220–224 (1997).
5. Tsodyks, M. V. & Markram, H. The neural code between neocortical pyramidal neurons depends on neurotransmitter release probability. *Proc. Natl Acad. Sci. USA* **94,** 719–723 (1997).
6. Lee, A. *et al.* Ca^{2+}/calmodulin binds to and modulates P/Q-type calcium channels. *Nature* **399,** 155–159 (1999).
7. Lee, A., Scheuer, T. & Catterall, W. A. Ca^{2+}/calmodulin-dependent facilitation and inactivation of P/Q-type Ca^{2+} channels. *J. Neurosci.* **20,** 6830–6838 (2000).
8. Peterson, B. Z., DeMaria, C. D., Adelman, J. P. & Yue, D. T. Calmodulin is the Ca^{2+} sensor for Ca^{2+}-dependent inactivation of L-type calcium channels. *Neuron* **22,** 549–558 (1999).
9. Chao, S. H., Suzuki, Y., Zysk, J. R. & Cheung, W. Y. Activation of calmodulin by various metal cations as a function of ionic radius. *Mol. Pharmacol.* **26,** 75–82 (1984).
10. Colecraft, H. M., Patil, P. G. & Yue, D. T. Differential occurrence of reluctant openings in G-protein-inhibited N- and P/Q-type calcium channels. *J. Gen. Physiol.* **115,** 175–192 (2000).
11. Zuhlke, R. D., Pitt, G. S., Deisseroth, K., Tsien, R. W. & Reuter, H. Calmodulin supports both inactivation and facilitation of L-type calcium channels. *Nature* **399,** 159–162 (1999).
12. Zuhlke, R. D., Pitt, G. S., Tsien, R. W. & Reuter, H. Ca^{2+}-sensitive inactivation and facilitation of L-type Ca^{2+} channels both depend on specific amino acid residues in a consensus calmodulin-binding motif in the α_{1C} subunit. *J. Biol. Chem.* **275,** 21121–21129 (2000).
13. Qin, N., Olcese, R., Bransby, M., Lin, T. & Birnbaumer, L. Ca^{2+}-induced inhibition of the cardiac Ca^{2+} channel depends on calmodulin. *Proc. Natl Acad. Sci. USA* **96,** 2435–2438 (1999).
14. Peterson, B. Z. *et al.* Critical determinants of Ca^{2+}-dependent inactivation within an EF-hand motif of L-type Ca^{2+} channels. *Biophys. J.* **78,** 1906–1920 (2000).
15. Houdusse, A. & Cohen, C. Target sequence recognition by the calmodulin superfamily: implications from light chain binding to the regulatory domain of scallop myosin. *Proc. Natl Acad. Sci. USA* **92,** 10644–10647 (1995).
16. Elshorst, B. *et al.* NMR solution structure of a complex of calmodulin with a binding peptide of the Ca^{2+} pump. *Biochemistry* **38,** 12320–12332 (1999).
17. Ehlers, M. D., Zhang, S., Bernhardt, J. P. & Huganir, R. L. Inactivation of NMDA receptors by direct interaction of calmodulin with the NR1 subunit. *Cell* **84,** 745–755 (1996).
18. Putkey, J. A., Sweeney, H. L. & Campbell, S. T. Site-directed mutation of the trigger calcium-binding sites in cardiac troponin C. *J. Biol. Chem.* **264,** 12370–12378 (1989).
19. Mori, M. *et al.* Novel interaction of the voltage-dependent sodium channel (VDSC) with calmodulin: does VDSC acquire calmodulin-mediated Ca^{2+}-sensitivity? *Biochemistry* **39,** 1316–1323 (2000).
20. Keen, J. E. *et al.* Domains responsible for constitutive and Ca^{2+}-dependent interactions between calmodulin and small conductance Ca^{2+}-activated potassium channels. *J. Neurosci.* **19,** 8830–8838 (1999).
21. Fanger, C. M. *et al.* Calmodulin mediates calcium-dependent activation of the intermediate conductance KCa channel, IKCal. *J. Biol. Chem.* **274,** 5746–5754 (1999).
22. Erickson, M. G. & Yue, D. T. FRET reveals tethering of calmodulin to calcium channel complex in single living cells. *Biophys. J.* **80,** 196a (2001).
23. Rodney, G. G. *et al.* Calcium binding to calmodulin leads to an N-terminal shift in its binding site on the ryanodine receptor. *J. Biol. Chem.* **276,** 2069–2074 (2001).
24. Barth, A., Martin, S. R. & Bayley, P. M. Specificity and symmetry in the interaction of calmodulin domains with the skeletal muscle myosin light chain kinase target sequence. *J. Biol. Chem.* **273,** 2174–2183 (1998).
25. Kink, J. A. *et al.* Mutations in paramecium calmodulin indicate functional differences between the C-terminal and N-terminal lobes in vivo. *Cell* **62,** 165–174 (1990).
26. Ohya, Y. & Botstein, D. Diverse essential functions revealed by complementing yeast calmodulin mutants. *Science* **263,** 963–966 (1994).
27. Sutton, K. G., McRory, J. E., Guthrie, H., Murphy, T. H. & Snutch, T. P. P/Q-type calcium channels mediate the activity dependent feedback of syntaxin-1A. *Nature* **401,** 800–804 (1999).
28. Kincaid, R. L., Billingsley, M. L. & Vaughan, M. Preparation of fluorescent, cross-linking, and biotinylated calmodulin derivatives and their use in studies of calmodulin-activated phosphodiesterase and protein phosphatase. *Methods Enzymol.* **159,** 605–626 (1988).
29. Patil, P. G., Brody, D. L. & Yue, D. T. Preferential closed-state inactivation of neuronal calcium channels. *Neuron* **20,** 1027–1038 (1998).
30. Song, L. S., Sham, J. S., Stern, M. D., Lakatta, E. G. & Chang, H. Direct measurement of SR release flux by tracking 'Ca^{2+} spikes' in rat cardiac myocytes. *J. Physiol. (Lond.)* **512,** 677–691 (1998).

Supplementary information is available on *Nature*'s World-Wide Web site (http://www.nature.com) or as paper copy from the London editorial office of *Nature*.

Acknowledgements

We thank W. Agnew, C. Chen, H. Colecraft, M. Erickson, S. Takahashi, H. Agler and E. Sobie for discussion; B. Peterson for initial attempts to detect P/Q-type channel facilitation; and T. Snutch for the gift of human α_{1A} clone. This work was supported by an NIH NRSA fellowship (C.D.D.) and grants from the NIH (D.T.Y.) and NNI (T.W.S.).

Correspondence and requests for materials should be addressed to D.T.Y. (e-mail: dyue@bme.jhu.edu).

B cells acquire antigen from target cells after synapse formation

Facundo D. Batista, Dagmar Iber & Michael S. Neuberger

Medical Research Laboratory of Molecular Biology, Hills Road, Cambridge, CB2 2QH, UK

Soluble antigen binds to the B-cell antigen receptor and is internalized for subsequent processing and the presentation of antigen-derived peptides to T cells[1]. Many antigens are not soluble, however, but are integral components of membrane; furthermore, soluble antigens will usually be encountered *in vivo* in a membrane-anchored form, tethered by Fc or complement receptors[2–4]. Here we show that B-cell interaction with antigens that are immobilized on the surface of a target cell leads to the formation of a synapse and the acquisition, even, of membrane-integral antigens from the target. B-cell antigen receptor accumulates at the synapse, segregated from the CD45 co-receptor which is excluded from the synapse, and there is a corresponding polarization of cytoplasmic effectors in the B cell. B-cell antigen receptor mediates the gathering of antigen into the synapse and its subsequent acquisition, thereby potentiating antigen processing and presentation to T cells with high efficacy. Synapse formation and antigen acquisition will probably enhance the activation of B cells at low antigen concentration, allow context-dependent antigen recognition and enhance the linking of B- and T-cell epitopes.

To investigate the B-cell response to antigen encountered as part of an immune complex tethered to a cell surface, immune complexes comprising hen-egg lysozyme (HEL) aggregated with specific immunoglobulin-γ (IgG) monoclonal antibodies were loaded on to the surface of an Fcγ receptor (FcγR)-expressing myeloid cell line. The immune complexes had a patchy distribution over the myeloid cell surface (Fig. 1a, b); however, on incubation with antigen-specific B cells, cell aggregates were formed in which the immune complexes on the myeloid cell and the B-cell antigen receptor (BCR) on the B cell were gathered together into a region of synapsis (Fig. 1c, d).

Similar results were obtained using immune complexes loaded onto FcγRI-expressing L-cell transfectants. Immunocytochemistry suggested that there is a gathering of tethered immune complexes, mediated by the BCR (possibly aided by the oligomeric nature of the BCR[5]) and accompanied by an apparent reorganization of the B-cell surface, as judged by segregation of the BCR from CD45 in the region of synapsis (Fig. 1e).

This concentration of BCR is reminiscent of the capping of surface IgM that results from incubation of B cells with polyvalent anti-IgM antisera[6,7]. We therefore determined whether the reorganization of the B cell depended on the polyvalent nature of the immune complex. We generated transfectants displaying HEL antigen as a presumptively monovalent integral membrane antigen and used one of these transfectants (J[mHEL]6; Fig. 2a) in excess as a target for HEL-specific B cells. Confocal microscopy showed that, after 10 min, most B cells were in conjunction with a target; BCR was concentrated in the region of synapsis but with clear exclusion of CD45 (Fig. 2b, c, f; Supplementary Information movie 1).

Reorganization of components of the B-cell membrane was also evident from a depletion of CD22 from the centre of most synapses (although often concentrated at the edges), where there was a concentration of ganglioside GM1 (which is associated classically with many Src-family tyrosine kinases). There was also polarization of cytoplasmic components, as judged by a depletion of the signal-inhibitory phosphatase SHP1 in the region of the synapse (Fig. 2d–f), but a concentration of phosphotyrosine-containing proteins as well

as actin and phospholipase C (PLC)-γ2 (Fig. 2d). This gross reorganization of a B cell after interacting with a target cell may reflect changes that also occur (but possibly on a smaller scale) after BCR crosslinking by soluble antigen, as such crosslinking[8,9] leads to BCR translocation into a GM1-enriched fraction that is depleted of CD22 and CD45.

We wanted to determine whether reorganization of the B cell could be detected using targets displaying a lower density of a lower-affinity antigen. Transfectants expressing a membrane-integral form of a mutated HEL (mHEL*) that exhibits a 100-fold reduced affinity for the HyHEL10 BCR[10] were screened for low-expressing clones: J[mHEL*]8 displays only around 9×10^3 mHEL* molecules per cell (compared with J[mHEL]6, which expresses about 4×10^5 mHEL per cell).

After incubation of J[mHEL*]8 with HEL-specific B cells, staining for mHEL* (which was previously only dim) was now brightly focused in the synapse (Fig. 3a). This quantity of mHEL* antigen is only sufficient to bring a small proportion of the total BCR into the synapse; however, there is nevertheless a local reorganization of the B cell as the BCR gathering is accompanied by local exclusion of CD45. Notably, the low abundance of mHEL* on the target cell surface is sufficient to trigger B-cell activation, as judged by the upregulation of CD86. Indeed, surface-tethered mHEL* is several orders of magnitude more efficacious than soluble HEL* in this respect (Fig. 3b, c). This is consistent with the apparent increased potency of membrane (as opposed to soluble) antigens in determining B-cell fate *in vivo*[11,12], which probably reflects the effective affinity increase resulting from restricting antigen mobility to two dimensions, coupled with the ability to concentrate antigen into the synapse[13].

To follow synapse formation in real time and exclude the possibility of a fixation artefact, we established targets that displayed mHEL fused to green fluorescent protein (GFP). Incubation with HEL-specific B cells led to rapid aggregation of mHEL–GFP in the synapse (Fig. 3d), although the frequency of synapses decreased at later time points (data not shown). The B cells bind well to their targets even at 13 °C, but formation of a synapse at which BCR and antigen have visibly accumulated requires a higher temperature—consistent with a need for membrane reorganization (Fig. 3e). Similar kinetics of synapse formation were also observed in a different B-cell/target interaction system—that of B cells carrying the 3-83 BCR specific for major histocompatability complex (MHC) class I molecules with targets that express H2-K^b (Fig. 3f; BCR/antigen affinity estimated[14] to be about $10^5\,M^{-1}$).

We wondered whether the decrease in observable synapses over time reflected internalization or degradation of antigen–BCR. In T cells, rapid internalization of the antigen receptor is observed after their interaction with antigen-presenting cells[15]. After culturing HEL-specific B cells with mHEL targets, flow cytometry showed that there was a rapid downregulation of BCR on the surface of the sorted B cells—more rapid than with soluble antigen (Fig. 4a, b).

This downregulation was peculiar to the BCR and did not apply to the CD19, CD22 or CD45 co-receptors; in addition, experiments performed using B-cell transfectants rather than splenic B cells showed that the downregulation occurring with the antigen-specific BCR did not extend to an irrelevant BCR expressed on the same cell (Fig. 4c). This loss of detectable surface BCR might reflect its internalization by the B cell, its acquisition by the target cell or some form of masking. Immunocytochemistry of cells sorted after co-culture showed that IgM was readily detectable in the sorted B cells (but not the sorted target cells), if they were permeabilized before staining (Fig. 4d). This IgM is unlikely to be *de novo* synthesized IgM that has not yet been transported to the cell surface, as protease stripping of surface IgM on splenic HEL-specific B cells showed that the intracellular pool of IgM was very small. Moreover, co-staining for IgM and HEL showed that, after B-cell–mHEL target interaction, the permeabilized, sorted B cells stained brightly for the

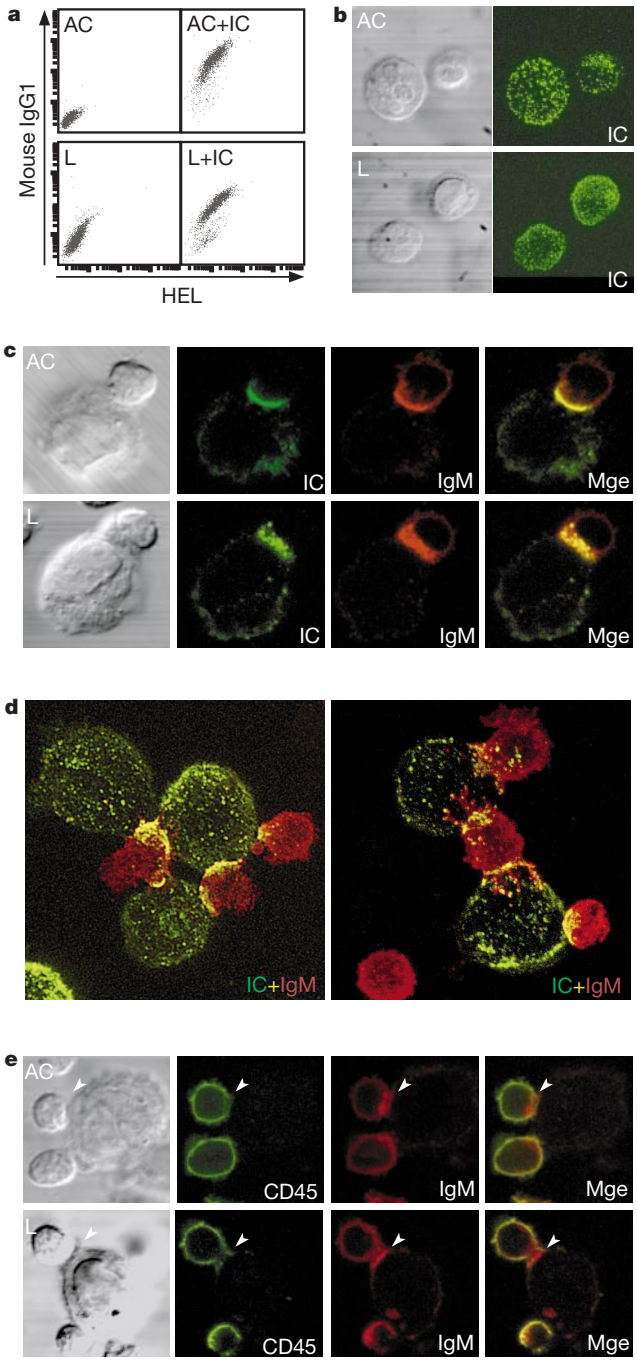

Figure 1 Synapse formation between B cell and antigen-displaying target cell. **a**, Loading of HEL–IgG immune complexes (ICs) onto the 279.AC1 myeloid cell line[27] or L-cell transfectants expressing human FcγRI. ICs were detected by staining for HEL and IgG1. L, L cells; AC, 279.AC1 cells. **b**, ICs are patchily distributed on the surface of 279.AC1 (top) or L[FcγRI] cells (bottom) that have been loaded at 4 °C, fixed and stained for mouse IgG1. Projection views are shown on right. **c**, Synapse formation after incubation (10 min, 37 °C) of IC-loaded targets with excess HEL-specific splenic B cells. For both myeloid and L cells, a single optical section of a single B-cell/target cell interaction is shown in either single or merged view. Whereas most B cells were in contact with a target when IC-loaded L[FcγRI] cells were used, only 10% of the B cells formed aggregates with IC-loaded 279.AC1 cells, correlating with internalization of the ICs at 37 °C by the myeloid cells—reflecting their expression of FcγRII and FcγRIII (not shown). **d**, Projection views of HEL-specific splenic B cells interacting with IC-loaded L[FcγRI] cells. Cells were double stained with anti-mouse IgG1 (for ICs; green) and anti-mouse IgM (for BCR; red). **e**, Comparison of BCR (red) and CD45R(B220) (green) distribution on HEL-specific B cells interacting with IC-loaded 279.AC1 or L[FcγRI] targets; a single optical section is shown in each case.

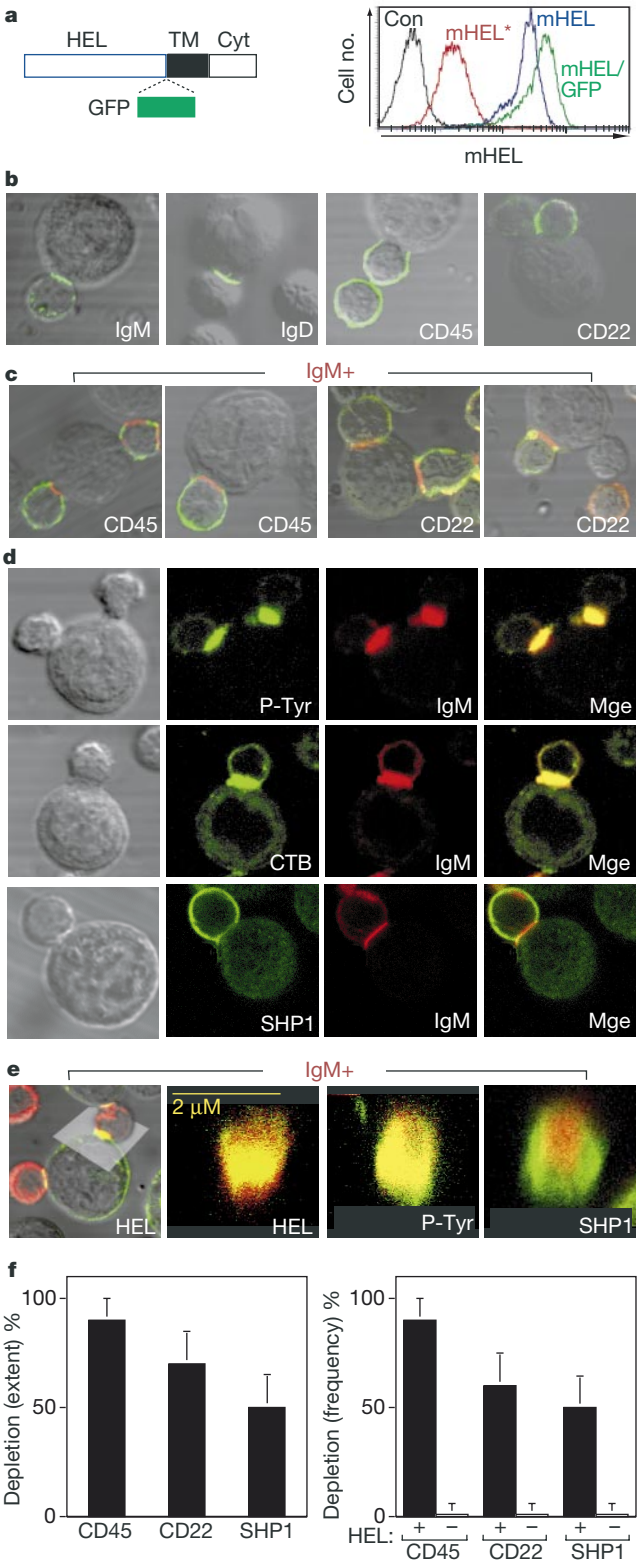

Figure 2 Polarization of the B cell after encountering membrane-immobilized antigen. **a**, Abundance of surface HEL in the cloned J558 transfectants (J[mHEL]6, J[mHEL*]8 and J[mHEL–GFP]) monitored by staining with anti-HEL IgG1-κ (HyHEL5) and PE-conjugated anti-κ. **b**, Distribution of BCR (IgM or IgD), CD22 and CD45 on HEL-specific splenic B cells interacting with J[mHEL]6 targets viewed as single optical sections. Cells were fixed after a 10-min incubation at 37 °C. **c**, Segregation of IgM from CD45 and CD22. Samples were prepared as in **a** but co-stained for CD45 or CD22 (green) and IgM (red). **d**, Polarization of HEL-specific B cells interacting with J[mHEL]6 targets analysed by double staining, in each case showing a single confocal section in single or merged view. Ganglioside GM1 was detected using cholera toxin B subunit (CTB). See Supplementary Information for additional staining for actin and PLC-γ2. **e**, Views along the plane of synapsis co-staining for IgM (red) and HEL, phosphotyrosine or SHP1 (green), showing coincidence of HEL–IgM and phosphotyrosine–IgM at the synapse but exclusion of SHP1. **f**, Quantification of the depletion of CD45, CD22 and SHP1 at synapses. Left, the mean extent of depletion of the appropriate marker at the synapse (from analysis of an average of 50 synapses) is expressed relative to the abundance of that marker adjacent to the synapse but in the same confocal plane. Right, the percentage of antigen-specific synapses ('HEL+') in which such depletion was noted (CD45, below 80%; CD22 and SHP1, below 60%) is compared with depletion in contacts between B cells and antigen-lacking targets ('HEL–').

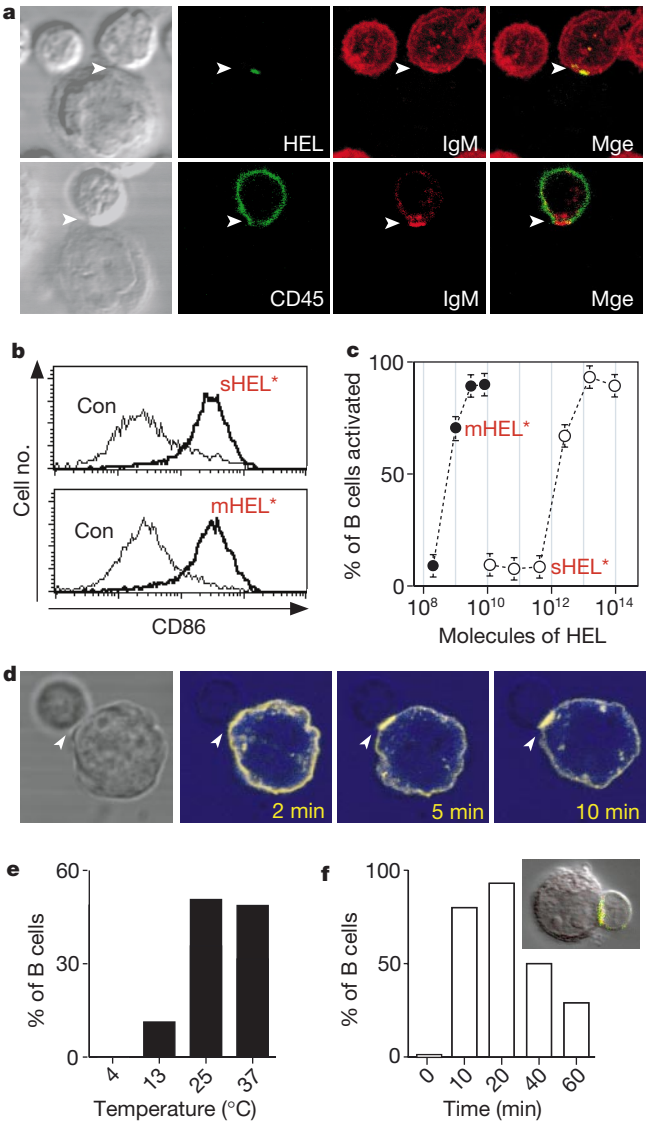

Figure 3 Parameters affecting synapse formation. **a**, Synapse formation between HEL-specific splenic B cells and J[mHEL*]8 targets (see Fig. 2a), which express antigen of reduced affinity at low density. Top, single or merged view of cells stained for HEL and IgM. Bottom, staining for CD45 and IgM, showing a single optical section. **b**, Culture of HEL-specific splenic B cells (20 h) with either J[mHEL*]8 (twofold excess) or soluble HEL (0.1 μg ml^{-1}) causes similar B-cell activation as judged by upregulation of CD86. **c**, Comparison of B-cell activation by membrane-tethered and soluble HEL. HEL-specific splenic B cells were cultured with varying concentrations of soluble HEL* or varying numbers of J558[mHEL*] targets, and activation was monitored as the percentage of B cells with upregulated expression of CD86. **d**, Real-time microscopy of an HEL-specific splenic B cell interacting at 20 °C with an mHEL–GFP-expressing target. **e**, Temperature dependence of synapse formation, as judged by the percentage of B cells bound to a target in which 50% of the IgM in one optical section was concentrated in the region of synapsis. **f**, Synapse frequency as a function of time. The experiment shown (as in **e** but at 37 °C) was performed using H2K^b-specific splenic B cells from 3-83 mice and H2K^b hybridoma targets. Shown is a single-plane confocal image of such a synapse (co-stained for IgM, red; H2K^b, green).

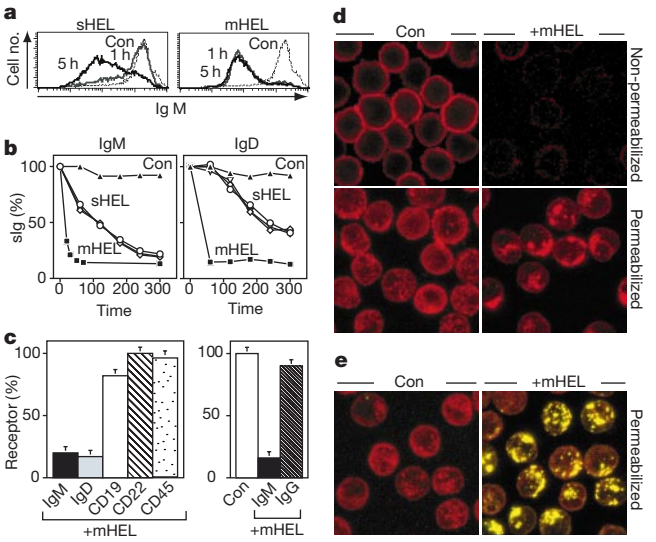

Figure 4 Downregulation of surface BCR after antigen encounter. **a**, Downregulation of IgM on HEL-specific splenic B cells after incubation (1 or 5 h at 37 °C) with saturating (10 μg ml^{-1}) amounts of soluble HEL or J[mHEL]6 target cells. Thin line indicates unstimulated cells. After incubation, cells were analysed by flow cytometry, gating on scatter and CD45R(B220) expression. **b**, Surface IgM and IgD expression on HEL-specific splenic B cells as a function of incubation time at 37 °C with J[mHEL]6 targets (filled boxes), control targets (untransfected J558; filled triangles) or soluble HEL (at 10, 1 and 0.1 μg ml^{-1}; open symbols). Surface immunoglobulin (sIg) expression at each time point is presented as the percentage mean surface immunoglobulin fluorescence relative to that of untreated cells. **c**, Antigen-specific BCR and not CD19, CD22, CD45 or an irrelevant BCR is downregulated. Left, expression of the indicated markers was monitored on HEL-specific splenic B cells after a 1-h incubation at 37 °C with J[mHEL]6 targets. Right, surface IgM and IgG2a expression was monitored in a parallel experiment but using mouse B-lymphoma transfectants[30] that co-express an HEL-specific IgM and a non-HEL-specific IgG2a BCR. Con, IgM expression after with incubation with untransfected J558 targets. **d**, Downregulated surface IgM can be revealed by permeabilization treatment of the B cell. HEL-specific splenic B cells were incubated at 37 °C for 1 h with J[mHEL]6 targets (or untransfected J558 controls, left), sorted on the basis of scatter and CD45R(B220) expression, fixed, and subjected or not to permeabilization treatment before staining with anti-IgM (red) and analysis by immunofluorescence microscopy. **e**, HEL colocalizes with downregulated IgM in the B cell. Samples as in **d** but stained for HEL (green) and IgM (red).

antigen, indicating that downregulation of the BCR might reflect acquisition of the antigen from the target cell and internalization of the mHEL–BCR complex by the B cell (Fig. 4e).

If the B cell acquires the antigen from the target cell, this should be visible in living cells using mHEL–GFP targets, without the risk of flow cytometry or fixation-associated artefacts. This is indeed the case. Following the interaction at 20 °C in real time shows that synapse formation is followed by the appearance of GFP fluorescence at points in the B cell that are distant from the synapse (Fig. 5a); this effect is more marked if the cells are incubated at 37 °C (Fig. 5b). Furthermore, if these cells are fixed and permeabilized, antigen transfer is evident from the fact that serial sections reveal co-localization of mHEL–GFP and IgM at sites in the B cell that are both removed from, and in a different plane to that of the synapse (Fig. 5c; Supplementary Information movie 2). The mHEL–GFP that has transferred to the B cell seems to undergo degradation, as the GFP fluorescence of the B cell diminishes with time (Fig. 5d).

The ability of the B cell to acquire an integral membrane antigen from the target cell and then internalize and degrade it should presumably allow the B cell to present antigen-derived peptides to T cells. HEL-specific B-cell transfectants co-cultured with MHC class-II-negative mHEL targets are very effective in presenting HEL-derived peptides to T cells (Fig. 5e). This presentation does not simply reflect BCR-mediated uptake of soluble mHEL fragments that have been released spontaneously by the target cells, as presentation is abolished if the B cells and target cells are separated by a mesh.

This presentation of membrane-tethered antigens is impressively efficient: co-incubation of 10^5 HEL-specific B cells with only 3×

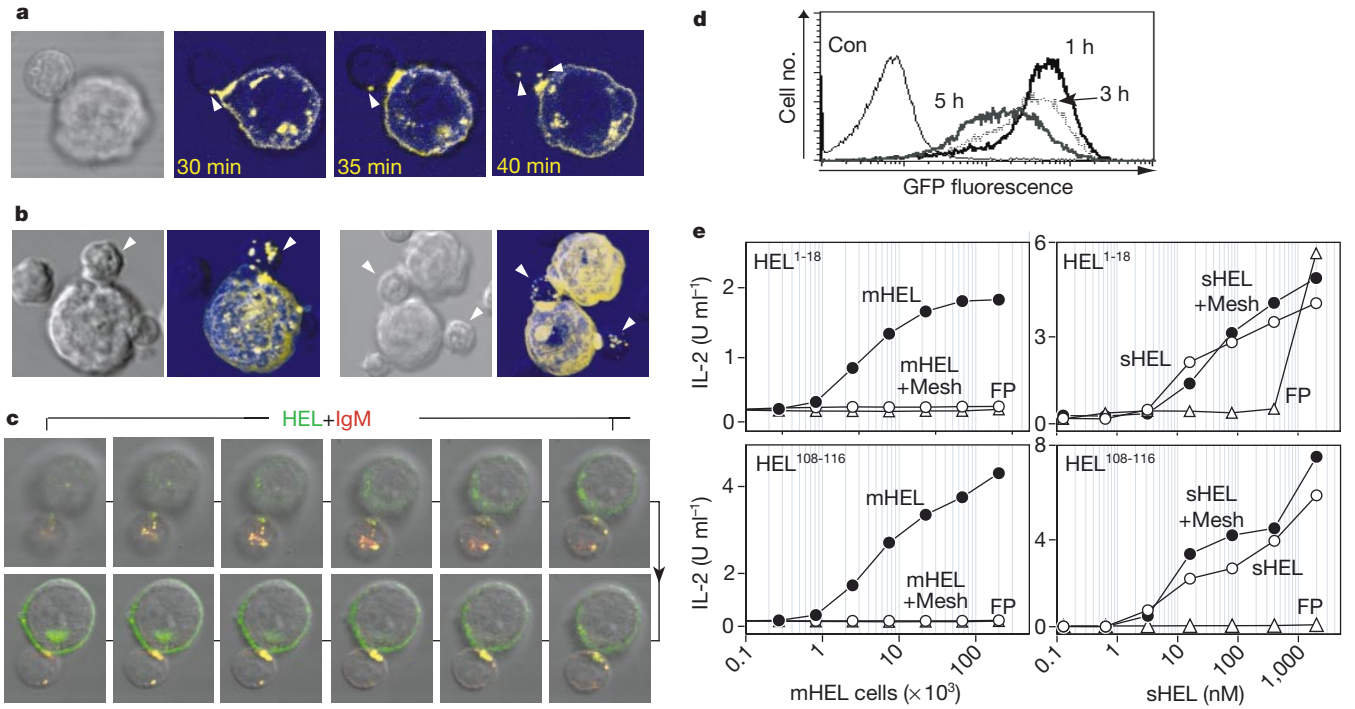

Figure 5 B cells acquire and present integral membrane antigens from the target cell. **a**, Real-time microscopy (single optical section) of an HEL-specific splenic B cell interacting with an mHEL–GFP target at 20 °C. **b**, Two examples of antigen acquisition from an mHEL–GFP target showing live cells (projection views) after a 40-min incubation at 37 °C. **c**, Serial optical sections of a fixed and permeabilized HEL-specific splenic B cell (smaller cell) interacting with a J[mHEL]6 target, showing HEL (green)/BCR (red) colocalization at sites in the B cell distant from the synapse. **d**, GFP fluorescence diminishes with time in HEL-specific splenic B cells incubated with J[mHEL/GFP] targets. GFP fluorescence in scatter and B220-gated B cells was monitored after 1, 3 and 5 h of incubation with targets. **e**, Presentation of HEL-derived epitopes to T cells by HEL-specific B-cell transfectants incubated with either J[mHEL]6 targets (left) or soluble HEL (right). B cells (10^5) and target cells (or soluble HEL, as indicated) were cultured (0.3 ml) with T-cell hybridomas specific for HEL^{1-18} or $HEL^{108-116}$ in the context of MHC class II molecules with, in some cases (open symbols), the target cells separated from the B cell/T cell mix by a mesh (0.2-μm Anopore membrane; Nunc). T-cell activation was monitored by measuring IL-2 production after 24 h. FP, fluid phase presentation by B cells lacking an HEL-specific BCR.

10^3 mHEL-expressing target cells (which correspond to a total of some 10^8–10^9 surface-expressed mHEL molecules) is sufficient to yield detectable interleukin (IL)-2 production in the antigen-presentation assay. In contrast, presentation of soluble HEL under similar assay conditions requires more than 10^{11} molecules of antigen. The increased efficacy of presentation of tethered (as opposed to soluble) antigen is even more striking when using mutated HELs exhibiting lower affinity for the BCR (data not shown).

The precise nature of the synapse is at present unclear, although co-staining with clathrin and early endosomal antigen suggests that much of the BCR–antigen complex may be internalized at the synapse (data not shown). Nevertheless, the synapse formed between the B cell and the antigen-displaying target cell shares some obvious similarities to the synapse formed between T cells and their targets, such as a concentration of antigen receptor but exclusion of CD45 from the region of synapsis[16–19]. But whereas T cells recognize antigen displayed in the context of MHC on many autologous cell types, it would seem beneficial if B-cell activation by antigen displayed on autologous cells were biased towards antigens tethered by professional receptors (such as FcR or CD21) and against abundant membrane antigens of self. One might imagine that there are surface glycoproteins on autologous cells that mediate selective recruitment of appropriate BCR co-receptors into (or out of) the synapse and thereby bias B-cell activation to FcR/CD21-tethered antigens.

The BCR-mediated concentration of antigen into the synapse is followed by antigen acquisition. Acquisition of an integral membrane protein from a target cell is not without precedent[20–22], although the mechanism remains unknown. Proteolytic release of the antigen from the target remains a possibility, but our failure to detect such proteolysis[23] leads us to favour a BCR-mediated pinching of membrane vesicles from the target cell. Our results show that the acquisition allows extremely efficient antigen presentation, which probably not only reflects the actual acquisition of the antigen: the gathering of BCR and the resultant polarization of the B cell may also enhance the antigen processing machinery of the B cell[24–26]. Together with the fact that membrane tethering of antigen also leads to great enhancement of B-cell signalling, as judged by the upregulation of CD86 (Fig. 3c), it seems that the focusing of antigen into the synapse may be important in B-cell responses to antigen—especially at low antigen abundance. With respect to membrane-integral antigens on foreign target cells, the gathering of antigen into the synapse and its consequent acquisition will presumably enhance the extent to which cognate B cells will present peptides to T cells that are derived from proteins linked to the antigen recognized by the BCR (rather than from irrelevant proteins in the foreign target). This might favour efficient recruitment of T-cell help and bias against promiscuous T-cell activation and the development of autoimmunity. □

Methods

Loading and detection of immune complexes

To load immune complexes onto 279.AC1 myeloid cells[27] or L-cell transfectants expressing human FcγRI (a gift from M. Clark), we incubated cells as described[23] with a mixture of biotinylated-HEL, HEL-specific IgG1 HyHEL5 and F10 (which recognize HEL epitopes distinct from that recognized by the HyHEL10 BCR expressed by B cells from MD4 transgenic mice) and rabbit anti-mouse IgG. Loaded immune complexes were detected using fluorescein isothiocyanate (FITC)–streptavidin and PE-conjugated goat anti-mouse IgG1. We detected SHP1 and phosphorylated tyrosine (P-Tyr) using rabbit polyclonal antisera (SantaCruz) and biotinylated monoclonal antibody 4G10 (Upstate Biotechnol-

ogy), respectively. Staining specificity was controlled by single staining, as well as by using secondary antibodies in the absence of the primary stain.

Generation of target cells

Target cells displaying a membrane-integral version of either wild-type HEL or a mutant[10] exhibiting reduced affinity for HyHEL10 ([R^{21}, D^{101}, G^{102}, N^{103}] designated HEL*) were generated by transfecting mouse J558L plasmacytoma cells with constructs analogous to those used[10] for expression of soluble HEL/HEL*, except that 14 Ser/Gly codons, the $H2K^b$ transmembrane region, and a 23-codon cytoplasmic domain were inserted immediately upstream of the termination codon by polymerase chain reaction. For mHEL–GFP, we included the EGFP coding domain in the Ser/Gly linker. Abundance of surface HEL was monitored by flow cytometry and radiolabelled-antibody binding using HyHEL5 and D1.3 HEL-specific monoclonal antibodies, for which the mutant HELs used in this work show unaltered affinities[10].

Interaction assays

For B-cell/target interaction assays, splenic B cells from 3-83 or MD4 transgenic mice[28,29] carrying (IgM + IgD) BCRs specific for HEL or $H2K^k$/$H2K^b$were freshly purified on Lympholyte and incubated with a twofold excess of target cells in RPMI, 50 mM HEPES pH 7.4, for the appropriate time at 37 °C before being applied to polylysine-coated slides. Cells were fixed in 4% paraformaldehyde/PBS or methanol and permeabilized with PBS/0.1% Triton X-100 before immunofluorescence. We acquired confocal images using a Nikon E800 microscope attached to BioRad Radiance Plus scanning system equipped with 488-nm and 543-nm lasers, as well as differential interference contrast for transmitted light. GFP fluorescence in living cells in real time was visualized using a Radiance 2000 and Nikon E300 inverted microscope. Images were processed using BioRad Lasersharp 1024 or 2000 software to provide single plane images, confocal projections or slicing.

Antigen presentation

Presentation of HEL epitopes to T-cell hybridomas 2G7 (specific for $I\text{-}E^k[HEL^{1-18}]$) and 1E5 (specific for $I\text{-}E^d[HEL^{108-116}]$) by transfectants of the LK35.2 B-cell hybridoma expressing an HEL-specific IgM BCR was monitored as described[10].

Received 12 December 2000; accepted 30 March 2001.

1. Lanzavecchia, A. Antigen-specific interaction between T and B cells. *Nature* **314,** 537–539 (1985).
2. Klaus, G. G., Humphrey, J. H., Kunkl, A. & Dongworth, D. W. The follicular dendritic cell: its role in antigen presentation in the generation of immunological memory. *Immunol. Rev.* **53,** 3–28 (1980).
3. Tew, J. G., Kosco, M. H., Burton, G. F. & Szakal, A. K. Follicular dendritic cells as accessory cells. *Immunol. Rev.* **117,** 185–211 (1990).
4. Kosco-Vilbois, M. H., Gray, D., Scheidegger, D. & Julius, M. Follicular dendritic cells help resting B cells to become effective antigen-presenting cells: induction of B7/BB1 and upregulation of major histocompatibility complex class II molecules. *J. Exp. Med.* **178,** 2055–2066 (1993).
5. Schamel, W. W. & Reth, M. Monomeric and oligomeric complexes of the B cell antigen receptor. *Immunity* **13,** 5–14 (2000).
6. Taylor, R. B., Duffus, W. P. H., Raff, M. C. & de Petris, S. Redistribution and pinocytosis of lymphocyte surface immunoglobulin molecules induced by anti-immunoglobulin antibody. *Nature* **233,** 225–227 (1971).
7. Schreiner, G. F. & Unanue, E. R. Capping and the lymphocyte: models for membrane reorganisation. *J. Immunol.* **119,** 1549–1551 (1977).
8. Cheng, P. C., Dykstra, M. L., Mitchell, R. N. & Pierce, S. K. A role for lipid rafts in B cell antigen receptor signaling and antigen targeting. *J. Exp. Med.* **190,** 1549–1560 (1999).
9. Weintraub, B. C. *et al.* Entry of B cell receptor into signaling domains is inhibited in tolerant B cells. *J. Exp. Med.* **191,** 1443–1448 (2000).
10. Batista, F. D. & Neuberger, M. S. Affinity dependence of the B cell response to antigen: a threshold, a ceiling, and the importance of off-rate. *Immunity* **8,** 751–759 (1998).
11. Nemazee, D. & Burki, K. Clonal deletion of B lymphocytes in a transgenic mouse bearing anti-MHC class I antibody genes. *Nature* **337,** 562–566 (1989).
12. Hartley, S. B. *et al.* Elimination from peripheral lymphoid tissues of self-reactive B lymphocytes recognizing membrane-bound antigens. *Nature* **353,** 765–769 (1991).
13. Dustin, M. L. *et al.* Low affinity interaction of human and rat T cell adhesion molecule CD2 with its ligands aligns adhering membranes to achieve high physiological affinity. *J. Biol. Chem.* **272,** 30889–30898 (1997).
14. Lang, J. *et al.* B cells are exquisitely sensitive to central tolerance and receptor editing by ultralow affinity, membrane-bound antigen. *J. Exp. Med.* **184,** 1685–1697 (1996).
15. Valitutti, S., Muller, S., Cella, M., Padovan, E. & Lanzavecchia, A. Serial triggering of many T-cell receptors by a few peptide–MHC complexes. *Nature* **375,** 148–151 (1995).
16. Monks, C. R., Freiberg, B. A., Kupfer, H., Sciaky, N. & Kupfer, A. Three-dimensional segregation of supramolecular activation clusters in T cells. *Nature* **395,** 82–86 (1998).
17. Wulfing, C. & Davis, M. M. A receptor/cytoskeletal movement triggered by costimulation during T cell activation. *Science* **282,** 2266–2269 (1998).
18. Grakoui, A. *et al.* The immunological synapse: a molecular machine controlling T cell activation. *Science* **285,** 221–227 (1999).
19. Leupin, O., Zaru, R., Laroche, T., Muller, S. & Valitutti, S. Exclusion of CD45 from the T-cell receptor signaling area in antigen-stimulated T lymphocytes. *Curr. Biol.* **10,** 277–280 (2000).
20. Cagan, R. L., Kramer, H., Hart, A. C. & Zipursky, S. L. The bride of sevenless and sevenless interaction: internalization of a transmembrane ligand. *Cell* **69,** 393–399 (1992).
21. Huang, J. F. *et al.* TCR-mediated internalization of peptide–MHC complexes acquired by T cells. *Science* **286,** 952–954 (1999).
22. Hwang, I. *et al.* T cells can use either T cell receptor or CD28 receptors to absorb and internalize cell surface molecules derived from antigen-presenting cells. *J. Exp. Med.* **191,** 1137–1148 (2000).
23. Batista, F. D. & Neuberger, M. S. B cells extract and present immobilized antigen: implications for affinity discrimination. *EMBO J.* **19,** 513–520 (2000).
24. Casten, L. A., Lakey, E. K., Jelachich, M. L., Margoliash, E. & Pierce, S. K. Anti-immunoglobulin augments the B-cell antigen-presentation function independently of internalization of receptor-antigen complex. *Proc. Natl Acad. Sci. USA* **82,** 5890–5894 (1985).
25. Siemasko, K., Eisfelder, B. J., Williamson, E., Kabak, S. & Clark, M. R. Signals from the B lymphocyte antigen receptor regulate MHC class II containing late endosomes. *J. Immunol.* **160,** 5203–5208 (1998).
26. Serre, K. *et al.* Efficient presentation of multivalent antigens targeted to various cell surface molecules of dendritic cells and surface Ig of antigen-specific B cells. *J. Immunol.* **161,** 6059–6067 (1998).
27. Green, S. M., Lowe, A. D., Parrington, J. & Karn, J. Transformation of growth factor-dependent myeloid stem cells with retroviral vectors carrying c-myc. *Oncogene* 737–751 (1989).
28. Russell, D. M. *et al.* Peripheral deletion of self-reactive B cells. *Nature* **354,** 308–311 (1991).
29. Goodnow, C. C. *et al.* Altered immunoglobulin expression and functional silencing of self-reactive B lymphocytes in transgenic mice. *Nature* **334,** 676–682 (1988).
30. Aluvihare, V. R., Khamlichi, A. A., Williams, G. T., Adorini, L. & Neuberger, M. S. Acceleration of intracellular targeting of antigen by the B-cell antigen receptor: importance depends on the nature of the antigen-antibody interaction. *EMBO J.* **16,** 3553–3562 (1997).

Supplementary information is available on *Nature*'s World-Wide Web site (http://www.nature.com) or as paper copy from the London editorial office of *Nature*.

Acknowledgements

We thank B. Amos and S. Reichelt for help and advice with confocal microscopy, and S. Munro for helpful discussions. We are indebted those who provided antibodies, transgenic mice and cell lines. F.D.B. and D.I. were supported by the Arthritis Research Campaign and Studienstiftung des deutschen Volkes, respectively.

Correspondence and requests for materials should be addressed to F.D.B. (e-mail:fdb@mrc-lmb.cam.ac.uk) or M.S.N. (e-mail:msn@mrc-lmb.cam.ac.uk)

Duplexes of 21–nucleotide RNAs mediate RNA interference in cultured mammalian cells

Sayda M. Elbashir*, Jens Harborth†, Winfried Lendeckel*, Abdullah Yalcin*, Klaus Weber† & Thomas Tuschl*

** Department of Cellular Biochemistry; and † Department of Biochemistry and Cell Biology, Max-Planck-Institute for Biophysical Chemistry, Am Fassberg 11, D-37077 Göttingen, Germany*

RNA interference (RNAi) is the process of sequence-specific, post-transcriptional gene silencing in animals and plants, initiated by double-stranded RNA (dsRNA) that is homologous in sequence to the silenced gene[1–4]. The mediators of sequence-specific messenger RNA degradation are 21- and 22-nucleotide small interfering RNAs (siRNAs) generated by ribonuclease III cleavage from longer dsRNAs[5–9]. Here we show that 21-nucleotide siRNA duplexes specifically suppress expression of endogenous and heterologous genes in different mammalian cell lines, including human embryonic kidney (293) and HeLa cells. Therefore, 21-nucleotide siRNA duplexes provide a new tool for studying gene function in mammalian cells and may eventually be used as gene-specific therapeutics.

Uptake of dsRNA by insect cell lines has previously been shown to 'knock-down' the expression of specific proteins, owing to sequence-specific, dsRNA-mediated mRNA degradation[6,10–12]. However, it has not been possible to detect potent and specific RNA interference in commonly used mammalian cell culture systems, including 293 (human embryonic kidney), NIH/3T3 (mouse fibroblast), BHK-21 (Syrian baby hamster kidney), and CHO-K1 (Chinese hamster ovary) cells, applying dsRNA that varies in size between 38 and 1,662 base pairs (bp)[10,12]. This apparent lack of RNAi in mammalian cell culture was unexpected, because RNAi exists in mouse oocytes and early embryos[13,14], and because RNAi-related, transgene-mediated co-suppression was also observed in cultured Rat-1 fibroblasts[15]. But it is known that dsRNA in the cytoplasm of mammalian cells can trigger profound physiological